Identification of Surface Species on Titania-Supported Manganese, Chromium, and Copper Oxide Low-Temperature SCR Catalysts

Donovan A. Peña,[†] Balu S. Uphade,[‡] Ettireddy P. Reddy,[†] and Panagiotis G. Smirniotis*[,†]

Chemical and Materials Engineering Department, University of Cincinnati, Cincinnati, Ohio 45221-0012, and National Chemical Laboratory (NCL), Dr. Homi Bhabha Road, Pune−411 008, India

Received: December 11, 2003; In Final Form: April 6, 2004

TiO_2-supported transition metal oxides (Mn, Cr, and Cu) for the SCR of NO with NH_3 have been synthesized by wet impregnation. The adsorption and coadsorption of NH_3, NO, and O_2, in conjunction with in situ FT-IR spectroscopy, was used to elucidate the reaction mechanism as the samples were heated from 323 to 673 K. While Cr was the only transition metal that generated significant amounts of Brønsted acidity, strong Lewis acid sites were present over all of the materials. The peak strength corresponding to the $\delta_s(NH_3)$ coordinated to Lewis acid sites decreased in the following order: Ti > Mn > Cr ∼ Cu. Similarly, the peak strength corresponding to the $\delta_{as}(NH_3)$ coordinated to Lewis acid sites decreased as follows: Mn > Cr ∼ Cu. Exposing the catalysts to oxygen before the introduction of NO did not impact the adsorption of NO as nitrates on the catalysts, suggesting that labile lattice oxygen plays an important role in the formation of nitrates. Three types of nitrates were observed after the adsorption of NO. Monodentate and bidentate nitrates formed on the surface of all the materials tested, while bridged nitrates only formed on CrO_x/TiO_2. The in situ FTIR data collected resulted in the development of a reaction mechanism for MnO_x/TiO_2. A combination of moderately strong monodentate and bidentate nitrate species, along with a split in the symmetric deformation of NH_3 coordinated to Lewis acid sites, appear to be important for high activity and selectivity. The peak resulting from the vibrational mode of ammonia adsorbed on Lewis acid sites, which is located at ∼1170 cm^{-1}, is believed to be important in facilitating hydrogen abstraction to form amide species that react with bidentate nitrates (1620 cm^{-1}). It is proposed that the reaction mechanism proceeds through the formation of nitrosamide and azoxy species, which most likely possess lifetimes as reaction intermediates that are too brief for detection. In contrast to MnO_x/TiO_2, the apparent participation of Brønsted acid sites for CrO_x/TiO_2 suggests that a different reaction pathway is involved for this catalyst.

Introduction

The selective catalytic reduction (SCR) of NO with NH_3 in excess oxygen is a well-established commercial technology using V_2O_5 and WO_3 (or MoO_3) supported on anatase TiO_2.[1−2] The catalyst was designed to operate at medium temperatures (573−673 K). Consequently, the catalyst should be placed immediately after the boiler or at some other location upstream of the desulfurizer and/or particulate control device to avoid costly reheating of the flue gas. However, placement at that location leads to catalyst deactivation and SO_2 oxidation in coal-fired utility plants because of the high concentrations of SO_2 and particulate matter. Efforts have been made to develop catalysts capable of operating at low temperatures (353−523 K)[3−9] so that the catalyst bed may be moved downstream of the desulfurizer and/or particulate control device in what is known as the tail end configuration.[10] At the tail end (353−523 K) the concentrations of SO_2 and particulate matter in the flue gas are drastically reduced, which will result in increased catalyst life and decreased oxidation of SO_2 to SO_3. Recently, novel MnO_x catalysts were developed[11] that provided high activity and nitrogen selectivity in the presence of 10 vol % water at low temperatures (373−473 K).

Extensive in situ FT-IR studies have been reported in the past over vanadia/titania catalysts using NH_3, NO and O_2 as probe molecules to understand the SCR reaction mechanism using NH_3,[12−20] and the major mechanisms proposed have been reviewed by Busca et al.[21] Most of the studies concluded that NH_3 was readily adsorbed, while NO could not be adsorbed on the surface of vanadium pentoxide in the absence of oxygen. Earlier studies also suggested that NH_3 was adsorbed on Brønsted (as NH_4^+) as well as Lewis (as NH_x-like species; $x = 1−3$) acid sites on V_2O_5/TiO_2. However, most of the studies concluded that surface Brønsted acid sites are important active sites for the SCR reaction.[12,15−18] Additionally, the SCR of NO with NH_3 has been reported to follow both Langmuir−Hinshelwood[12] and Eley−Rideal[13] type mechanisms.

In a series of papers, Busca and co-workers[21−23] reported FT-IR results from ammonia, hydrazine, and pyridine adsorption over various transition metals supported on anatase TiO_2. In contrast to the work primarily performed by Topsøe and co-workers,[2,16−19] Busca and co-workers[24] concluded that Brønsted acidity plays no role in either SCR or SCO after studying various catalysts, including V_2O_5/TiO_2. Although a great deal of literature is available on using FT-IR to study the adsorption and coadsorption of NH_3, NO, and O_2 on V_2O_5/TiO_2, few papers deal with other catalytic systems used in the SCR of NO with NH_3.[23,25−29] In addition to V_2O_5/TiO_2, other catalytic systems including $Mn/\gamma\text{-}Al_2O_3$[28,30] and chromia[25] have also been studied.

* To whom correspondence should be addressed. Telephone: (513) 556-1474. Fax: (513) 556-3473. E-mail: panagiotis.smirniotis@UC.EDU.
[†] University of Cincinnati.
[‡] National Chemical Laboratory (NCL).

10.1021/jp0313122 CCC: $27.50
Published on Web 06/19/2004

Since titania-supported Mn, Cr, and Cu were previously found to perform well at low temperature,[11] the aim of this study is to determine the types of adsorbed species resulting from the adsorption of NH_3 and NO and to understand their role in order to propose a mechanism for the SCR of NO using NH_3 at low temperature.

Experimental Section

The titania-supported catalysts were synthesized by wet impregnation from nitrates of Cr, Mn, and Cu.[11] In the present study, catalysts were calcined at 673 K for 2 h in an O_2/He mixture (4% O_2). The high surface area anatase TiO_2 (Hombikat UV 100) was obtained from Sachtleben Chemie. N_2 adsorption experiments were performed on a Micromeritics ASAP 2010 with prepurified helium and ultrahigh purity nitrogen supplied by Wright Brothers. The sample was degassed at 523 K under vacuum prior to analysis. The measured surface area, pore volume and pore diameter were 309 $m^2\ g^{-1}$, 0.7 $cm^3\ g^{-1}$, and 4.5 nm, respectively.

FT-IR spectra were recorded using a Bio-Rad (FTS-40). Circular self-supporting thin wafers (8 mm diameter) consisting of 8−20 mg of material were used for the study. The wafers were placed in a high-temperature cell with CaF_2 windows and purged with prepurified grade helium (30 mL min^{-1}) at 673 K for 2 h to remove any adsorbed impurities. The wafer was cooled to 323 K and a background spectrum was collected before any gas adsorption. After cooling, NH_3 (4.06% in He), NO (1% in He), or pure O_2 was introduced into the cell at 30 mL min^{-1} for 1 h at 323 K to ensure complete saturation of the sample. Physisorbed gas was removed by flushing the wafer with helium for at least 3 h at 323 K before proceeding. The same procedure was followed for the adsorption of multiple gases, as helium flowed for 3 h at 323 K between gas adsorption steps. FT-IR single beam spectra were normally collected after desorbing the adsorbed gas at temperatures ranging from 323 to 673 K in a continuous helium flow. Sixteen scans were averaged at 323 K for each normalized spectrum at a resolution of 2 cm^{-1}.

Results and Discussion

A number of FT-IR experiments were performed to gain a better understanding of molecular behavior on the surface of the low-temperature SCR catalysts. Ammonia, nitric oxide, oxygen and nitric oxide, and mixtures of ammonia and nitric oxide were introduced to the catalysts to acquire information about surface species. The adsorption of NH_3 provided information on the nature of acid sites present, and its presence as a function of temperature revealed the strength of the acid sites. Similarly, the adsorption of NO showed the kinds of species that could form on the surface of each catalyst tested, and increasing temperatures were used to judge the stability of these compounds. The influence of O_2 on the nature of NO adsorption was included because only weak interactions between NO and the catalyst surface have been reported in the absence of O_2.[28] The combinations of NH_3 and NO consisted of the introduction of NO to materials with preadsorbed NH_3 or the introduction of NH_3 to a catalyst with preadsorbed NO. In all of these cases, the disappearance and generation of peaks provided valuable insight and allowed the identification of species and possible intermediates.

Ammonia Adsorption. Figure 1 shows normalized FT-IR spectra after NH_3 adsorption. All data were collected after ammonia adsorption and subsequent flushing with helium at 323 K. It can be seen that NH_3 adsorbed onto both Lewis and

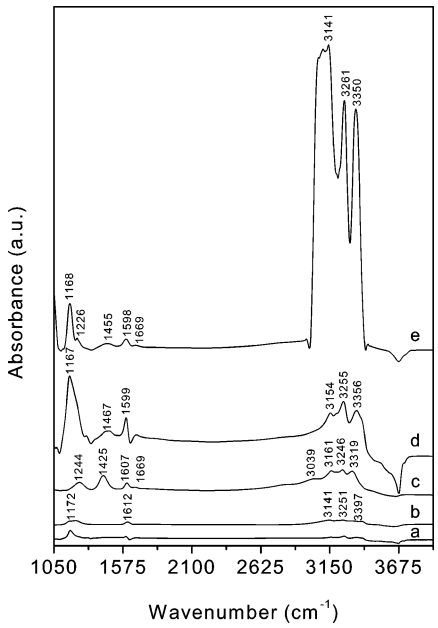

Figure 1. FTIR spectra of the adsorption of NH_3 on various catalysts at 323 K: (a) 20 wt % Mn/TiO_2; (b) 20 wt % Cu/TiO_2; (c) 20 wt % Cr/TiO_2; (d) 5 wt % Mn/TiO_2; (e) TiO_2.

Brønsted acid sites and was capable of forming amide species in some cases. The survival of the adsorbed species at elevated temperatures was used to compare the relative strength of different acid sites, and a detailed discussion for each oxide is presented below.

TiO_2. The catalyst support will be the first material discussed. Identifying species that form on the support is essential to isolating the effect different metal oxides have on the reactants. In the low wavenumber region, the TiO_2 support possesses bands at 1105, 1168, 1226, 1455, 1598, and 1669 cm^{-1}. The small peak at 1105 cm^{-1} corresponds to hydrogen bound to NH_3,[24] while the larger peaks at 1168 and 1226 cm^{-1} are a result of the symmetric deformation of NH_3 ($\delta_s(NH_3)$) coordinatively bound to Lewis acid sites.[31−32] There is a distinct possibility that NH_3 bound to the weaker acid sites may be in a more activated state to participate in SCR. This idea will resurface later in the discussion of NH_3 + NO adsorption on Mn/TiO_2. The formation of the weaker Lewis acid sites (1168 cm^{-1}) is attributed to the removal of water, while the stronger Lewis acid sites (1226 cm^{-1}) are generated from the removal of OH groups from the surface of TiO_2.[32] The small peak at 1105 cm^{-1} is due to weakly bound surface NH_3, as it disappears upon heating above 473 K. In contrast, the Lewis bound NH_3 represented by peaks at 1168 and 1226 cm^{-1} is strongly bound to the surface and remains present at 673 K. The band at 1598 cm^{-1} is attributed to the asymmetric deformation of NH_3 ($\delta_{as}(NH_3)$) coordinated to Lewis acid sites.[24,31] The peaks at 1455 and 1669 cm^{-1} correspond to the asymmetric and symmetric deformation of NH_4^+ ($\delta_{as}(NH_4^+)$ and $\delta_s(NH_4^+)$) bound to Brønsted acid sites, respectively.[20,31−32] The Brønsted acidity observed here may be attributed to the interaction between NH_3 and any adsorbed water that may have remained on the surface after heating or to impurities like SiO_2 that are capable of generating Brønsted acidity, as anatase titania has been reported to adsorb NH_3 in coordinated form over Lewis acid sites.[33] The latter case is most likely, as trace levels of metal oxide impurities were evident after EDAX analysis (not shown). The Brønsted acid sites represented by peaks at 1455 and 1669 cm^{-1} are moderately strong, as they were barely visible at 573 K. In the high wavenumber region, peaks are observed at 3141, 3261,

and 3350 cm^{-1}. The bands at 3141 and 3261 cm^{-1} can be assigned to symmetric stretching of NH_3 coordinated to Lewis acid sites ($\nu_s(NH_3)$), while the peak at 3350 cm^{-1} can be assigned to asymmetric stretching of NH_3 coordinated to Lewis acid sites ($\nu_{as}(NH_3)$).[20,33]

Mn/TiO$_2$. When 5 wt % Mn is added to the support, an important phenomenon occurs. In the low wavenumber region, 5 wt % Mn/TiO_2 has peaks at 1167, 1301, 1467, 1599, and 1680 cm.$^{-1}$ The peak at 1167 cm^{-1}, which is larger in 5 wt % Mn/TiO_2 than all of the other catalysts tested, grows significantly. This peak corresponds to $\delta_s(NH_3)$ coordinated to Lewis acid sites, which was earlier suggested to play an important role in low-temperature SCR. The band at 1301 cm^{-1} has also been assigned to $\delta_s(NH_3)$ coordinated to Lewis acid sites,[32] while those at 1467 and 1680 cm^{-1} were attributed to $\delta_{as}(NH_4^+)$ and $\delta_s(NH_4^+)$ bound to Brønsted acid sites, respectively, from the presence of impurities on the support[33] because manganese has not been found to generate Brønsted acid sites.[28] The peaks at 1167 and 1301 cm^{-1} began to decrease significantly at 573 K and almost disappeared at 673 K. Not only have the number of species attributed to $\delta_s(NH_3)$ increased compared to TiO_2, but also the weaker bond indicated by desorption at slightly lower temperatures indicates that manganese destabilizes the species as well. This could further activate the NH_3 to facilitate its participation in the SCR reaction. Meanwhile, the peaks at 1467 and 1680 cm^{-1} weaken and remain until 473 K before disappearing at 573 K. The remaining band at 1599 cm^{-1} is attributed to the asymmetric deformation of NH_3 ($\delta_{as}(NH_3)$) coordinated to Lewis acid sites.[24,31] The behavior of this peak identically follows the peak observed at 1167 cm^{-1}, which was discussed above. Bands in the high wavenumber region at 3154 and 3255 cm^{-1} are assigned to $\nu_s(NH_3)$ coordinated to Lewis acid sites, and the band at 3356 cm^{-1} is assigned to $\nu_{as}(NH_3)$ coordinated to Lewis acid sites.[20,33]

When the manganese content is increased to 20 wt %, the situation changes dramatically. Significantly smaller peaks are only present at the following four wavenumbers: 1174, 1596, 3257, and 3358 cm^{-1}. All four of these peaks correspond to the peaks observed in similar locations for the sample containing only 5 wt % Mn, which was described in the previous paragraph. The peak areas decrease as the metal loading increases because of the relationship between Mn and NH_3. MnO_x-TiO_2 was found to be highly active in oxidizing ammonia.[33] Consequently, much of the ammonia that does adsorb on the surface reacts to form oxidation products. This would account for the observations seen in this work, as much of the ammonia that adsorbed on the Lewis acid sites reacted and prevented the ability to draw meaningful conclusions. It is for this reason that additional data were collected using 5 wt % Mn/TiO_2 instead of 20 wt % Mn/TiO_2. The behavior of the peaks as the temperature increased was identical to that observed over 5 wt % Mn/TiO_2.

Cr/TiO$_2$. In the low wavenumber region, 20 wt % Cr/TiO_2 has peaks at 1244, 1425, 1607, and 1669 cm^{-1} that correspond to $\delta_s(NH_3)$ bound to Lewis acid sites,[33] $\delta_{as}(NH_4^+)$ bound to Brønsted acid sites,[24] $\delta_{as}(NH_3)$ coordinated to Lewis acid sites,[33] and $\delta_s(NH_4^+)$ bound to Brønsted acid sites,[33] respectively. Unlike the materials previously discussed, 20 wt % Cr/TiO_2 possesses a large number of Brønsted acid sites. The peaks at 1244 ($\delta_s(NH_3)$) and 1607 cm^{-1} ($\delta_{as}(NH_3)$) remain until 573 K but disappear after exposure to 673 K. The weaker peaks at 1425 ($\delta_{as}(NH_4^+)$) and 1669 cm^{-1} ($\delta_s(NH_4^+)$) are already absent at 573 K. Bands in the high wavenumber region are observed at 3039, 3161, 3246, and 3319 cm^{-1}. The band at 3039 cm^{-1} is attributed to the symmetric stretching of NH_4^+ bound to Brønsted acid sites ($\nu_s(NH_4^+)$),[20] while the two peaks at 3161 and 3246 cm^{-1} are attributed to $\nu_s(NH_3)$ coordinated to Lewis acid sites.[20,33] The final peak at 3319 cm^{-1} results from $\nu_{as}(NH_3)$ coordinated to Lewis acid sites.[20]

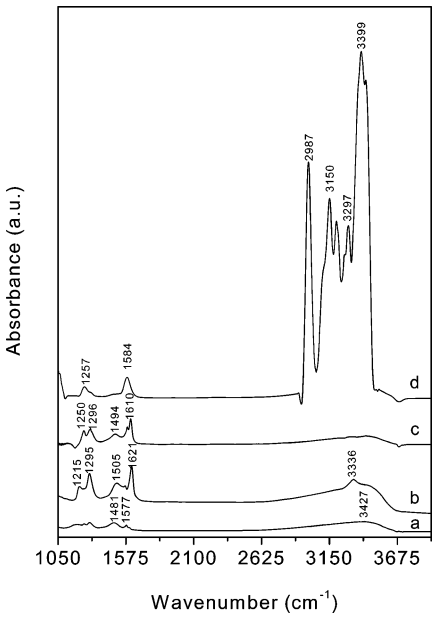

Figure 2. FTIR spectra of the adsorption of NO on various catalysts at 323 K: (a) 20 wt % Cu/TiO_2; (b) 20 wt % Cr/TiO_2; (c) 5 wt % Mn/TiO_2; (d) TiO_2.

Cu/TiO$_2$. In the low wavenumber region, 20 wt % Cu/TiO_2 has peaks at 1172, 1220, and 1612 cm^{-1}. The first two peaks are assigned to $\delta_s(NH_3)$ bound to Lewis acid sites,[34] while the last peak may be assigned to either $\delta_{as}(NH_3)$ coordinated to Lewis acid sites or possibly the scissoring of NH_2 associated with hydrazine adsorbed on the surface.[33-34] Since the different assignments[34] are only separated by 9 cm^{-1}, it is possible that the peak may contain contributions from both types of species. All three of the peaks observed at 1172, 1220, and 1612 cm^{-1} indicated fairly strong adsorption on the surface, as they all remain at 573 K before disappearing at 673 K. In the high wavenumber region, small peaks are visible at 3141, 3251, and 3397 cm^{-1}. The first two peaks can be assigned to $\nu_s(NH_3)$ coordinated to Lewis acid sites, while the last peak is attributed to $\nu_{as}(NH_3)$ coordinated to Lewis acid sites.[34]

Nitric Oxide Adsorption. The next set of experiments examined the surface of the materials after the adsorption of nitric oxide, which is the other reactant in SCR. Figure 2 shows the FT-IR spectra of the TiO_2 support, 5 wt % Mn/TiO_2, 20 wt % Cr/TiO_2, and 20 wt % Cu/TiO_2. All data presented were collected after the adsorption of NO and subsequent flushing with helium at 323 K. The introduction of NO led to the formation of a number of peaks. While it has been reported that temperatures below 273 K are required to study metal−NO complexes,[35-36] the nitrate species observed in this work at 323 K suggest that mobile lattice oxygen on the surface of the mixed oxides are responsible for the adsorption. Since the catalytic performance of these materials was determined in excess oxygen,[11] the effect of oxygen on nitric oxide adsorption was investigated (not shown). Neither the peak positions nor the intensities changed significantly in the presence of oxygen, and the intensities of the peaks formed were not affected by the time the materials were exposed to NO.

TiO$_2$. As in the case of NH_3 adsorption, the contribution of the catalyst support will be identified by examining the species capable of adsorbing on the surface of TiO_2 after exposure to

NO. Five peaks are present in the low wavenumber region of TiO_2 at 1160, 1257, 1302, 1492, and 1584 cm^{-1}. All four of these features are within the range 1625−1100 cm^{-1}. which corresponds to coordinated nitrates on TiO_2.[37] Within the nitrate category, the peak at 1160 cm^{-1} can be assigned to the stretching mode (υ(NO)) of the protonated anionic nitrosyl NOH species, and the combined peaks at 1257 and 1302 cm^{-1} can be assigned to monodentate nitrate species adsorbed on the surface of the TiO_2 support.[37] Similarly, the two peaks present at 1492 and 1584 cm^{-1} may be assigned to monodentate and bidentate nitrate species, respectively, on the surface of TiO_2.[37] All of the nitrate species observed were quite stable and remained on the surface until 673 K. In the high wavenumber region, a large number of intense peaks were present at 2987, 3150, 3203, 3297, 3399, and 3432 cm^{-1}. These intense peaks were only present on TiO_2, suggesting that the addition of transition metals covered the NO adsorption sites initially present on TiO_2. The peaks at 2987, 3150, and 3203 cm^{-1} could not be confidently assigned but may possibly be the result of O−H stretching in NOH groups that form on the particular TiO_2 used in this study. In other work,[37] peaks indicative of NOH groups have been observed near 3600 cm^{-1}. The shift to lower wavenumbers may be the result of the previously discussed impurities that are likely to be present on the surface of this particular TiO_2. The peaks present at 3297, 3399, and 3432 cm^{-1} are located at wavenumbers that correspond to the stretching of OH present in water (νOH) that may be adsorbed on the TiO_2 surface.[20,37] Nitric oxide likely adsorbs on the surface through disproportionation, which is the likely source of adsorbed water on the surface.[37] Now that the contributions from the support have been identified, the role of different mixed oxides will be discussed below.

Mn/TiO_2. Five peaks are present at 1250, 1296, 1494, 1584, and 1610 cm^{-1} in the low wavenumber region of 5 wt % Mn/TiO_2, while none of the peaks observed for TiO_2 are present in the high wavenumber region. This strongly suggests that a loading of 5 wt % Mn was enough to cover those particular TiO_2 sites capable of adsorbing NO. Similar to TiO_2, the peaks at 1250, 1296, and 1494 cm^{-1} can be assigned to monodentate nitrate species, while the remaining peaks at 1584 and 1610 cm^{-1} can be attributed to bidentate nitrate species.[37] All of the peaks reduce dramatically after reaching 573 K, and only a remnant of the peak at 1610 cm^{-1} remains at 673 K. Since all of the spectra have been normalized, the larger peaks in the low wavenumber region suggest that the addition of Mn to TiO_2 increases the number of NO adsorption sites relative to TiO_2 itself. It is interesting to note that the monodentate nitrates represented by the split peaks of 1250 and 1296 cm^{-1} shift to a higher wavenumber in comparison to TiO_2. Additionally, the lack of any peaks in the high wavenumber region suggests that Mn selectively binds to the sites of TiO_2 that are responsible for the peaks discussed in the previous paragraph.

Cr/TiO_2. More peaks are generated upon the addition of Cr to TiO_2. Examining the spectrum for 20 wt % Cr/TiO_2 shows the presence of five bands in the low wavenumber region, which are located at 1215, 1295, 1505, 1573, and 1621 cm^{-1}. The peaks at 1215 and 1295 cm^{-1} are assigned to monodentate nitrates, and the particular monodentate nitrate peak at 1295 cm^{-1} is the most intense for 20 wt % Cr/TiO_2. The previously observed bidentate nitrates are seen in peaks at 1505 and 1573 cm,$^{-1}$ while bridged nitrates are observed at 1621 cm^{-1}.[29, 37] At 473 K, all of the peaks have decreased in height and area significantly. Only the peaks at 1573 and 1621 cm^{-1} are visible at 573 K. The bidentate nitrates represented by the peak at 1573 cm^{-1} are very stable, as a small peak remains even at 673 K at a slightly lower wavenumber. The only distinguishable feature in the high wavenumber region is a peak located at 3336 cm^{-1}, which may indicate the formation of NOH groups.

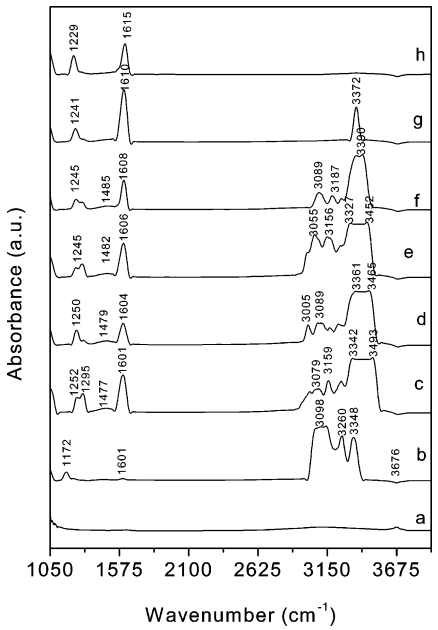

Figure 3. FTIR spectra of the adsorption and desorption of NH_3 and NO on TiO_2 at various temperatures: (a) TiO_2 in helium at 323 K; (b) NH_3 adsorbed on TiO_2 at 323 K; (c−h) NO adsorbed onto TiO_2 with preadsorbed NH_3 at (c) 323, (d) 373, (e) 423, (f) 473, (g) 573, and (h) 673 K.

Cu/TiO_2. The final catalyst to be discussed in this figure, 20 wt % Cu/TiO_2, has a number of weak peaks in the low wavenumber region located at 1197, 1254, 1293, 1481, 1577, and 1599 cm^{-1} that can all be assigned to adsorbed nitrate species that were discussed above. The peak at 1197 cm^{-1} only remains present up to 373 K, indicating that it is not very stable and potentially reactive. All of the remaining peaks are mostly unchanged when heated to 573 K before disappearing completely at 673 K. A broad feature in the high wavenumber region that reaches a maximum at 3427 cm^{-1} is also observed.

Adsorption of NH_3 Followed by NO. The following paragraphs discuss the FTIR spectra obtained from the combined adsorption of NH_3 and NO on the surface of TiO_2 and the metal oxides supported on TiO_2. In the first case (NH_3−NO), NH_3 is first adsorbed on the wafer before flushing with helium and then introducing NO. In a similar fashion, NO is first adsorbed on TiO_2 before flushing with helium and then introducing NH_3 in the second case (NO−NH_3). The last step in each case was flushing with helium for 3 h before scanning. The behaviors of the adsorbed species are shown as a function of temperature in all of the figures discussed below.

TiO_2. Figure 3 shows the FTIR data collected from TiO_2 after NH_3−NO adsorption as the temperature is increased from 323 to 673 K. The initial peaks resulting from the adsorption of NH_3 at 1172, 1226, and 1601 cm^{-1} correspond to the peaks previously identified in Figure 1. The peak at 1172 cm^{-1}, which corresponds to the low-frequency component of the split band resulting from $\delta_s(NH_3)$ coordinated to Lewis acid sites, immediately disappears upon introducing NO. The disappearance of this peak strongly suggests that NH_3 bound in this form is the activated form of ammonia that is capable of participating in low-temperature SCR. The monodentate nitrate species located at 1252, 1295, and 1477 cm^{-1} that are observed after the introduction of NH_3−NO at 323 K are similar to the bands observed after NO adsorption on TiO_2 in Figure 2. The

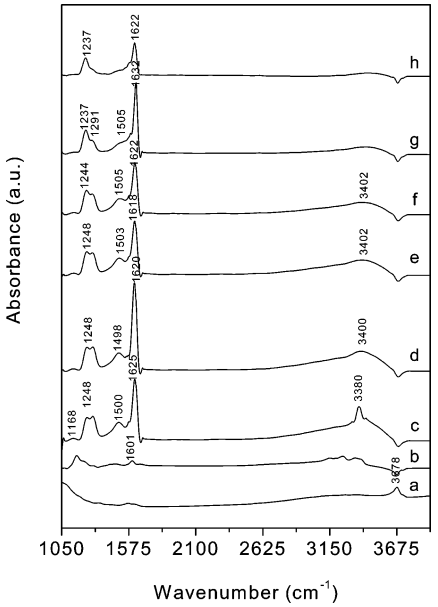

Figure 4. FTIR spectra of the adsorption and desorption of NH_3 and NO on 5 wt % Mn/TiO_2 at various temperatures: (a) 5 wt % Mn/TiO_2 in helium at 323 K; (b) NH_3 adsorbed on 5 wt % Mn/TiO_2 at 323 K; (c−h) NO adsorbed onto 5 wt % Mn/TiO_2 with preadsorbed NH_3 at (c) 323, (d) 373, (e) 423, (f) 473, (g) 573, and (h) 673 K.

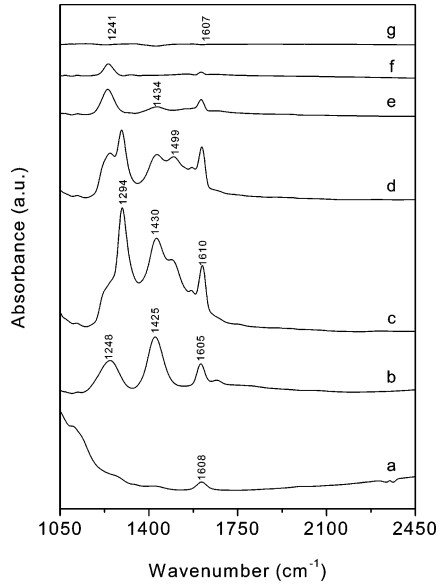

Figure 5. FTIR spectra of the adsorption and desorption of NH_3 and NO on 20 wt % Cr/TiO_2 at various temperatures: (a) 20 wt % Cr/TiO_2 in helium at 323 K; (b) NH_3 adsorbed on 20 wt % Cr/TiO_2 at 323 K; (c−h) NO adsorbed onto 20 wt % Cr/TiO_2 with preadsorbed NH_3 at (c) 323, (d) 373, (e) 423, (f) 473, (g) 573, and (h) 673 K.

monodentate nitrate species initially indicated by peaks at 1252 and 1295 cm^{-1} shift to lower wavenumbers as the temperature is increased, and the split in the peaks disappears as the temperature is raised above 573 K. In contrast, the monodentate species located at 1477 cm^{-1} have a weaker bond and disappear after heating at 573 K. The bidentate nitrates that form with NH_3 adsorbed on the surface appear at a higher wavenumber of 1601 cm^{-1} and gradually shift to higher wavenumbers with an increase in temperature. Since the $\delta_{as}(NH_3)$ peak initially present at 1601 cm^{-1} is very small, the increase in this peak upon the introduction of NO may be attributed to the formation of bridged nitrates and possibly the adsorption of water. Water may be generated by the SCR reaction between NH_3 and NO, the disproportionation of NO that was previously discussed, or the condensation of surface OH groups as the temperature is increased. The combination of these three effects may explain the erratic behavior of the 1601 cm^{-1} peak as the temperature increases. With the exception of the peak at 3372 cm^{-1}, all of the peaks in the high wavenumber region disappear upon reaching 573 K. This remaining peak lends support to the formation of water at higher temperatures, since adsorbed water is located near 3400 and 1630 cm^{-1} for V_2O_5/TiO_2 catalysts.[20] This is quite similar to the remaining peaks observed at 573 K near 1610 and 3372 cm^{-1}.

Mn/TiO_2. The situation changes when Mn is added to TiO_2. Figure 4 shows the FTIR data collected from Mn/TiO_2 after NH_3−NO adsorption as the temperature is increased from 323 to 673 K. Peaks are initially present at 1168, 1229, 1301, and 1601 cm^{-1} and correspond to the NH_3 species previously discussed in Figure 1. Peaks in the high wavenumber region similar to those observed in Figure 1 are also present at 3188, 3249, 3352, and 3395 cm^{-1}. After the introduction of NO the peak at 1168 cm^{-1} immediately disappears just as it did with the TiO_2 support discussed above, which lends further support to the idea that these are the active NH_3 species in the reaction. The immediate disappearance of IR peaks at 1168 cm^{-1}, which correspond to the NH_3 species was due to the shifting of NH_3 species from the catalyst surface to the monodentate NO species. While that peak disappeared, peaks were generated at 1144, 1248, 1292, 1500, 1625, and 3380 cm.$^{-1}$ The peak at 1144 cm^{-1} can be assigned to the formation of NO^- species on the surface of the catalyst.[37] While NO^- species that adsorb on Mn sites (1190 cm^{-1}) appear at a higher wavenumber than NO^- species that adsorb on TiO_2 (1150 cm^{-1}),[37] the lack of a peak near this location for TiO_2 in Figure 3 suggests that the peak observed in this work at 1144 cm^{-1} results from the formation of NO^- species on Mn sites. The peaks at 1248, 1292, and 1500 cm^{-1} correspond to the formation of monodentate nitrates that were discussed in detail in Figure 2. The largest peak, which occurs at 1625 cm^{-1}, results from the formation of the bridged nitrates that were discussed in Figure 2. The lone peak in the high wavenumber region occurs at 3380 cm^{-1}, which may be from water generated from the SCR reaction.

The NO^- species observed at 1144 cm^{-1} disappear after heating above 473 K, suggesting that this is a more reactive species because of its weaker bond. The monodentate nitrates located at 1248, 1292, and 1500 cm^{-1} are more strongly bound and remain on the surface until temperatures rise above 573 K. Out of the three peaks, the monodentate nitrate species indicated by the peak at 1248 cm^{-1} is the strongest because of its survival at temperatures as high as 673 K. The strength of the bridged nitrates formed at 1625 cm^{-1} is difficult to determine because of the overlapping water peak that appears in the same region. Water may be formed as a product of the SCR reaction that is occurring, or it may result from the condensation of OH groups on the catalyst surface. While NO^- species, monodentate nitrates, bidentate nitrates, bridged nitrates, and water are capable of forming on the catalyst surface after exposure to NH_3−NO, the ease of removal associated with NO^- species, monodentate nitrates represented by the peak at 1292 cm^{-1}, and possibly bidentate nitrates suggests that these species would be the most active in carrying out the SCR of NO.

Cr/TiO_2. After observation of the two similar cases discussed above, it was seen that the addition of Cr, which is the only transition metal tested that was capable of generating Brønsted acidity, yields different results. Figure 5 shows the FTIR data collected over 20 wt % Cr/TiO_2 after NH_3−NO adsorption as the temperature is increased from 323 to 673 K. The original

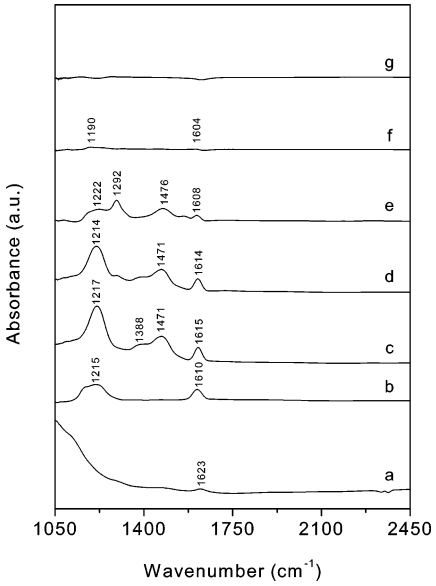

Figure 6. FTIR spectra of the adsorption and desorption of NH_3 and NO on 20 wt % Cu/TiO_2 at various temperatures: (a) 20 wt % Cu/TiO_2 in helium at 323 K; (b) NH_3 adsorbed on 20 wt % Cu/TiO_2 at 323 K; (c−h) NO adsorbed onto 20 wt % Cu/TiO_2 with preadsorbed NH_3 at (c) 323, (d) 373, (e) 423, (f) 473, (g) 573, and (h) 673 K.

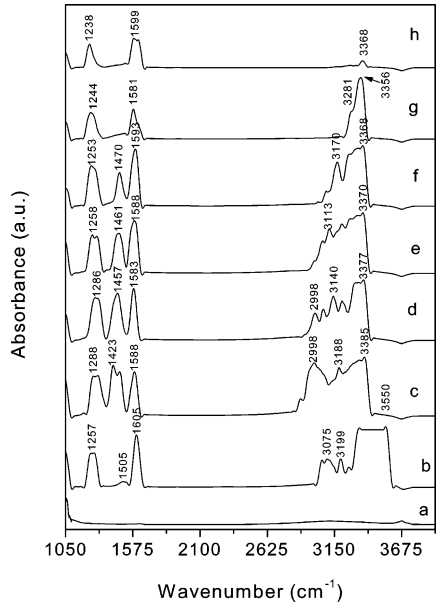

Figure 7. FTIR spectra of the adsorption and desorption of NO and NH_3 on TiO_2 at various temperatures: (a) TiO_2 in helium at 323 K; (b) NO adsorbed on TiO_2 at 323 K; (c−h) NH_3 adsorbed onto TiO_2 with preadsorbed NO at (c) 323, (d) 373, (e) 423, (f) 473, (g) 573, and (h) 673 K.

peaks observed after the introduction of NH_3 at 1248, 1425, 1605, and 1669 cm^{-1} correspond to the species that were previously discussed in Figure 1. In contrast to the results reported thus far, the peaks corresponding to NH_3 coordinated to Lewis acid sites do not immediately disappear upon introducing NO. In fact, they are still evident among the nitrate peaks that form, and it is the $\delta_s(NH_4^+)$ ions bound to Brønsted acid sites ($\sim$1609 cm^{-1}) that significantly decreased upon exposure to NO. After the introduction of NO, peaks were present at 1123, 1294, 1430, 1489, 1567, and 1610 cm.$^{-1}$ The peak at 1123 cm^{-1}, which only appears during the introduction of NO to preadsorbed NH_3, may be the result of chelated NO_2.[36] The peaks at 1294 and 1489 cm^{-1} can be assigned to the formation of monodentate nitrate species, while the peaks at 1567 and 1610 cm^{-1} can be attributed to adsorbed bidentate nitrate species. The peak located at 1430 cm^{-1} was attributed to ammonia bound to Brønsted acid sites. The monodentate nitrates indicated by the peak at 1294 cm^{-1} completely desorb from the surface at 473 K and reveal the presence of $\delta_s(NH_3)$ bound to Lewis acid sites at 1248 cm^{-1} that remain adsorbed until 673 K. The bidentate nitrates observed at 1567 cm^{-1} behave similarly to those observed at 1294 cm^{-1} and completely desorb at 473 K. Since the other peaks representing bidentate nitrates have disappeared after reaching 473 K, the band at 1607 cm^{-1} that remains above 473 K can most likely be attributed to the δ_{as}-(NH_3) coordinated to Lewis acid sites that are still adsorbed on the surface. Earlier, this peak was shown to survive until 673 K, and the superior size of the peak for bidentate nitrates prevented its observation until the nitrates desorbed. One important point to note is the lack of evidence for bridged nitrate formation in the presence of NH_3. Bridged nitrates were observed earlier in the discussion of Figure 2, when only NO was introduced.

Cu/TiO_2. Figure 6 shows the FTIR data collected over 20 wt % Cu/TiO_2 after NH_3−NO adsorption as the temperature is increased from 323 to 673 K. The original peaks observed after the introduction of NH_3 at 1167, 1215, and 1610 cm^{-1} correspond to the species that were previously discussed in Figure 1. Similar to what was observed for TiO_2 and 5 wt % Mn/TiO_2, the peak at 1167 cm^{-1}, which corresponds to $\delta_s(NH_3)$ coordinated to Lewis acid sites, immediately disappears upon exposure to NO. The effect is less noticeable in this case because the peak did not significantly split apart. After the introduction of NO, peaks were present at 1217, 1388, 1471, and 1615 cm^{-1}. The three peaks located at 1217, 1388, and 1471 cm^{-1} can only be generally categorized as oxidation products of NO[34] and are removed from the surface upon reaching 573 K. The exception is the peak at 1615 cm^{-1}, which can be attributed to a combination of $\delta_{as}(NH_3)$ and the scissoring of NH_2 species in hydrazine.[33−34] Any water that may have been generated as a result of the SCR reaction may also be contributing to this peak. This peak gradually weakens as the temperature rises and disappears upon reaching 573 K. This is the only case where no adsorbed species remained at only 573 K, as all of the other materials had peaks remaining at this temperature.

Adsorption of NO Followed by NH_3. TiO_2. As in the preceding sections, the presentation of results will begin with the support. Figure 7 shows the FTIR data collected from TiO_2 after NO−NH_3 adsorption as the temperature is increased from 323 to 673 K. The initial peaks collected at 323 K near 1257, 1505, and 1605 cm^{-1} correspond to the monodentate, bidentate, and bridged nitrate species, respectively, previously discussed in Figure 2. After exposure to NH_3 the peak at 1257 cm^{-1} shifts to 1288 cm^{-1}, while the peak at 1605 cm^{-1} shifts to 1588 cm^{-1}. Both of these peaks remain, even as the temperature is increased to 673 K. However, the peak at 1288 cm^{-1} moves down to 1238 cm^{-1} at 673 K. A new peak around 1460 cm^{-1} forms upon addition of NH_3 and disappears upon heating to 573 K. The location of this peak indicates $\delta_{as}(NH_4^+)$ bound to Brønsted acid sites,[32] and its behavior as a function of temperature is also consistent with that assignment. Consequently, this information suggests that NO is capable of forming NOH groups on the surface, which act as Brønsted acid sites. This is supported by the disappearance of the peak at 3550 cm,$^{-1}$ which is near the wavenumber assigned to OH stretching in NOH groups.[37] The peak at 3550 cm^{-1} disappears as the peak at 1460 cm^{-1} appears after the introduction of NH_3, suggesting that the NH_3 is binding to all of the NOH sites. Out of the many peaks

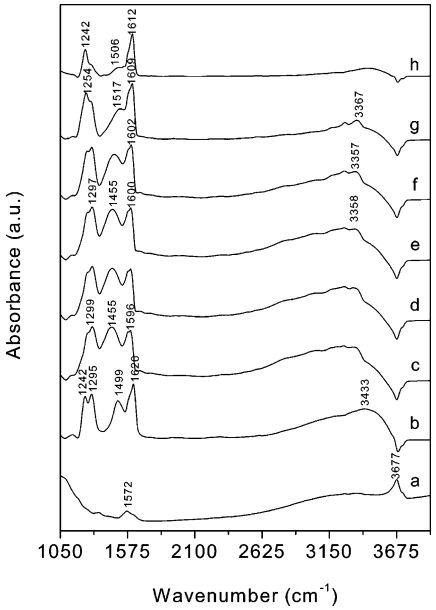

Figure 8. FTIR spectra of the adsorption and desorption of NO and NH_3 on 5 wt % Mn/TiO_2 at various temperatures: (a) 5 wt % Mn/TiO_2 in helium at 323 K; (b) NO adsorbed on 5 wt % Mn/TiO_2 at 323 K; (c−h) NH_3 adsorbed onto 5 wt % Mn/TiO_2 with preadsorbed NO at (c) 323, (d) 373, (e) 423, (f) 473, (g) 573, and (h) 673 K.

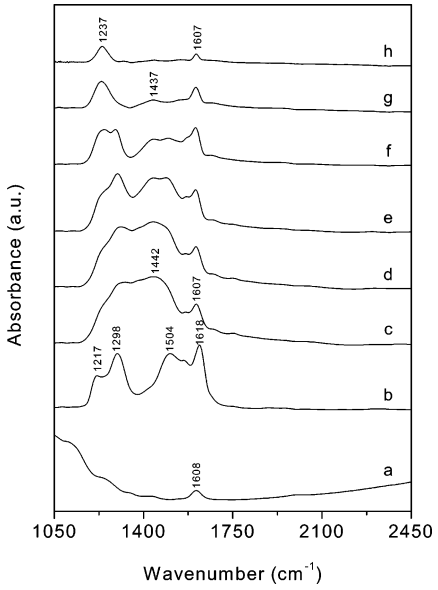

Figure 9. FTIR spectra of the adsorption and desorption of NO and NH_3 on 20 wt % Cr/TiO_2 at various temperatures: (a) 20 wt % Cr/TiO_2 in helium at 323 K; (b) NO adsorbed on 20 wt % Cr/TiO_2 at 323 K; (c−h) NH_3 adsorbed onto 20 wt % Cr/TiO_2 with preadsorbed NO at (c) 323, (d) 373, (e) 423, (f) 473, (g) 573, and (h) 673 K.

present in the high wavenumber region, the peak near 3368 cm^{-1} is the only one remaining at 673 K.

Mn/TiO_2. Figure 8 shows the FTIR data collected over 5 wt % Mn/TiO_2 after NO−NH_3 adsorption as a function of temperature. The initial peaks present at 1144, 1242, 1295, 1499, and 1620 cm^{-1} correspond to the NO^- species, monodentate nitrates, and bidentate nitrates that were explained in the discussion of Figure 2. The NO^- species, indicated by the peak at 1144 cm^{-1}, decreased in area and shifted to slightly higher wavenumbers after the introduction of NH_3 as the temperature increased to 573 K before disappearing entirely at 673 K. The monodentate nitrate species, indicated by split peaks at 1242 and 1295 cm^{-1}, shifted to lower wavenumbers and remained adsorbed on the surface at temperatures as high as 673 K. Any monodentate nitrate species that were present at 1499 cm^{-1} were unable to be observed because of adsorption of NH_3 on NOH Brønsted acid sites at 1455 cm^{-1}, which was explained in more detail during the discussion of TiO_2. The increase in wavenumber of this peak at temperatures above 423 K can be interpreted as the desorption of NH_3 from the NOH Brønsted acid sites, which allows the monodentate nitrates still adsorbed on the surface to be observed at wavenumbers closer to the original location of 1499 cm^{-1}. The bidentate nitrate species located at 1620 cm^{-1} are strongly bound to the surface and persist even at 623 K. Some smaller peaks in the high wavenumber region at 3167, 3273, and 3367 cm^{-1} become more resolved as the temperature increases to 573 K.

The absence of any peaks for water is a distinguishing feature in this case that supports our mass spectroscopy data (not shown) that show the absence of N_2 generation when NH_3 is introduced over Mn/TiO_2 with preadsorbed NO on the surface. The formation of NOH groups generates Brønsted acid sites that could potentially assist the activation of NH_3 to more readily participate in the SCR reaction. However, that clearly is not the case at these operating conditions. The monodentate and bidentate nitrates formed in this case are strongly bound to the surface, as they survive at temperatures of 673 K, and therefore, they are unlikely candidates to participate in the SCR reaction. All of these data strongly support the idea that adsorbed NH_3 reacts with gas-phase or weakly bound NO to carry out the SCR reaction at low temperature.

Cr/TiO_2. Continuing the discussion of Brønsted acid sites, Figure 9 shows the FTIR data collected over 20 wt % Cr/TiO_2, which possessed a significant amount of Brønsted acidity, after NO−NH_3 adsorption as the temperature is increased from 323 to 673 K. The original peaks observed after the introduction of NO at 1217, 1298, 1504, 1560, and 1618 cm^{-1} correspond to the species that were previously discussed in Figure 2. After the introduction of NH_3, a broad feature with peaks at 1323 and 1442 cm^{-1} was present along with peaks at 1564 and 1607 cm^{-1}. The lack of distinct features at 323 K for wavenumbers below 1500 cm^{-1} makes it difficult to identify the individual species present. However, the peaks visible at 1564 and 1607 cm^{-1} indicate the presence of bidentate nitrates and $\delta_{as}(NH_3)$ coordinated to Lewis acid sites. The picture is much clearer at 473 K, where distinct peaks are visible at 1245, 1290, 1442, 1500, 1576, and 1604 cm^{-1}. While both monodentate nitrates and $\delta_s(NH_3)$ may be overlapping to form the peak at 1245 cm^{-1}, the continued presence of this peak at 673 K and its downward shift to 1237 cm^{-1} confirm the presence of $\delta_s(NH_3)$. It is interesting to note that the peak at 1237 cm^{-1} and the one at 1607 cm^{-1}, which indicates the presence of $\delta_{as}(NH_3)$ coordinated to Lewis acid sites, remain on the surface at 673 K in the presence of NO. These same species only remained on the surface at 573 K when just NH_3 was introduced, indicating that the presence of adsorbed NO species increases the bond strength of NH_3 bound to Lewis acid sites. The peak at 1290 cm^{-1}, indicative of monodentate nitrate species, disappears above 473 K. The peak at 1442 cm^{-1}, representing $\delta_{as}(NH_4^+)$ bound to Brønsted acid sites, remains until 573 K, which is similar to the behavior observed in the absence of NO. The peaks at 1500 and 1576 cm^{-1} disappear at 573 K and are assigned to bidentate nitrates.

Cu/TiO_2. The broad peaks observed for 20 wt % Cu/TiO_2 in Figure 10 made the assignment of species difficult, especially since the peaks formed did not directly correspond to those that formed when only NH_3 or NO was adsorbed on the surface of

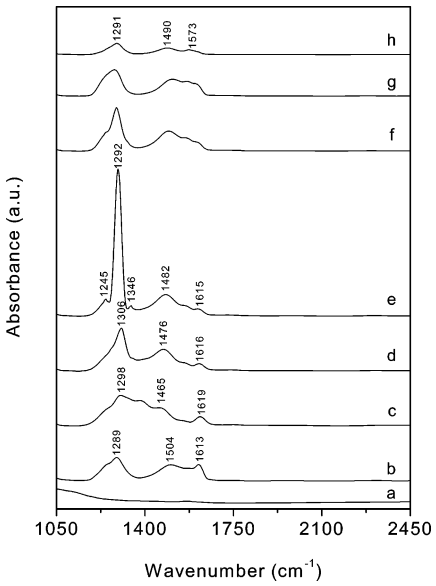

Figure 10. FTIR spectra of the adsorption and desorption of NO and NH_3 on 20 wt % Cu/TiO_2 at various temperatures: (a) 20 wt % Cu/TiO_2 in helium at 323 K; (b) NO adsorbed on 20 wt % Cu/TiO_2 at 323 K; (c−h) NH_3 adsorbed onto 20 wt % Cu/TiO_2 with preadsorbed NO at (c) 323, (d) 373, (e) 423, (f) 473, (g) 573, and (h) 673 K.

the catalyst. The original peaks observed after the introduction of NO at 1289, 1504, and 1613 cm^{-1} correspond to the species that were previously discussed in Figure 2. After the introduction of NH_3, a broad feature with peaks at 1298, 1387, and 1465 cm^{-1} appeared, and the peak at 1613 cm^{-1} shifted slightly upward to 1619 cm.$^{-1}$ The peak at 1292 cm^{-1} reaches its maximum at 423 K, suggesting that a reaction intermediate may be developing at this location. This peak appears in the general range where oxidation products of NO appear and is close to the peak at 1293 cm^{-1} that was present when only NO was adsorbed. Most of the other peaks present at 1482, 1562, and 1615 cm^{-1} remain present even at 673 K, suggesting that they may not be readily available to participate in the SCR reaction.

Reaction Mechanism. During the FTIR experiments focusing on the adsorption of NH_3, four species worthy of discussion formed. First, the symmetric deformation of NH_3 ($\delta_s(NH_3)$) coordinated to Lewis acid sites was observed over all of the materials studied. The relative strength of this species, which was determined by the desorption temperature, decreased in the following order: Ti > Mn > Cr ∼ Cu. However, it is important to note that this peak splits into two contributions over all of the materials studied except for Cr. It is the split peak located at the lower wavenumber (∼1167 cm^{-1}) that forms prominently over 5 wt % Mn/TiO_2 and is believed to play a major role in low-temperature SCR. Second, the asymmetric deformation of NH_3 ($\delta_{as}(NH_3)$) coordinated to Lewis acid sites was observed over all of the materials except TiO_2, and the relative strength of this species decreased in the following order: Mn > Cr ∼ Cu. The third and fourth species indicated by the asymmetric and symmetric deformations of NH_4^+ ($\delta_{as}(NH_4^+)$ and $\delta_s(NH_4^+)$) bound to Brønsted acid sites were observed over TiO_2, 5 wt % Mn/TiO_2, and 20 wt % Cr/TiO_2. Out of the transition metals studied, only Cr is known to generate Brønsted acidity, and the appearance of this species in the other materials was attributed to the presence of impurities. The relative strength of both these species decreased in the following order: Ti > Mn ∼ Cr. This result was significant because the Brønsted acid sites generated by the impurities on the support were stronger than those generated by the addition of Cr.

When only NO was adsorbed on the samples and examined by FTIR, the three species observed in this study were all nitrates even though oxygen was absent. Monodentate nitrates formed on the surface of all the materials, and the relative strengths decreased in the following order: Ti > Mn ∼ Cu > Cr. Bidentate nitrates were also observed over all of the materials tested, and the corresponding bond strengths decreased in the following order: Ti > Mn ∼ Cr > Cu. Finally, bridged nitrates only formed on the surface of 20 wt % Cr/TiO_2. A combination of moderate strength monodenate and bidentate species, which were observed over 5 wt % Mn/TiO_2, appear to be related to good catalytic activity and selectivity in low-temperature SCR.

After the reference spectra were collected over all of the materials for each of the reactants, NO was introduced to a sample with preadsorbed NH_3 to try and observe the reaction intermediates that form. The immediate disappearance of some NH_3 peaks after the introduction of NO was due to the shifting of NH_3 species from the catalyst surface to the NO species. This phenomenon will occur because of the bond between NH_3 species and Mn is weaker than the bond between Mn and NO species. Therefore, whenever NO is introduced after NH_3 adsorption, the rearrangement of NH_3 species will take place from catalyst surface to the monodentate NO species. The generation of water provides evidence that the SCR reaction occurred during the course of these experiments. It is essential to note that one particular peak (∼ 1170 cm^{-1}) corresponding to the symmetric deformation of NH_3 ($\delta_s(NH_3)$) coordinated to Lewis acid sites immediately disappeared upon exposure to NO, suggesting that it is this type of NH_3 that participates in the SCR reaction. Specifically, it was the low wavenumber contribution of the split peak corresponding to $\delta_s(NH_3)$ coordinated to Lewis acid sites that disappeared for TiO_2, Mn/TiO_2, and Cu/TiO_2. This particular species was absent over Cr/TiO_2 and could not participate in the reaction. In contrast to all of the other materials studied, it was the peak corresponding to the symmetric deformation of NH_4^+ ($\delta_s(NH_4^+)$) bound to Brønsted acid sites that immediately disappeared after the introduction of NO, which suggests that a different pathway may be involved for supported oxides of Cr. Lewis acid sites appear to play an important role in activating NH_3 to participate in the SCR reaction for TiO_2, Mn/TiO_2, and Cu/TiO_2, while Brønsted acid sites appear to be crucial for Cr/TiO_2.

Reversing the order of gases introduced to the sample produced opposite results. Mass spectroscopy experiments that introduced NH_3 to Mn/TiO_2 preadsorbed with NO and the failure to observe water peaks in the FTIR spectra demonstrate that the SCR reaction does not proceed, indicating that the reaction initiates with the adsorption of NH_3 on the catalyst surface. Overall, the identification of peaks and their corresponding species was difficult during this series of experiments because of the overlapping features encountered. It proved especially difficult to identify species on 20 wt % Cu/TiO_2. NOH species were able to form on the surface of TiO_2 and Mn/TiO_2, which allowed the formation of species corresponding to the asymmetric deformation of NH_4^+ ($\delta_{as}(NH_4^+)$) bound to Brønsted acid sites after exposure to NH_3. Brønsted acid sites also formed over Cr/TiO_2, but it was already shown to have them in Figure 1 when only NH_3 was introduced. The strength of the Brønsted acid sites decreased in the following order: Cr > Ti > Mn. Strongly bound nitrate species, whose likelihood of reacting with NH_3 is diminished by such a strong bond to the surface, formed over all of the materials studied, supporting the claim that the reaction initiates with the adsorption of NH_3 on the catalyst.

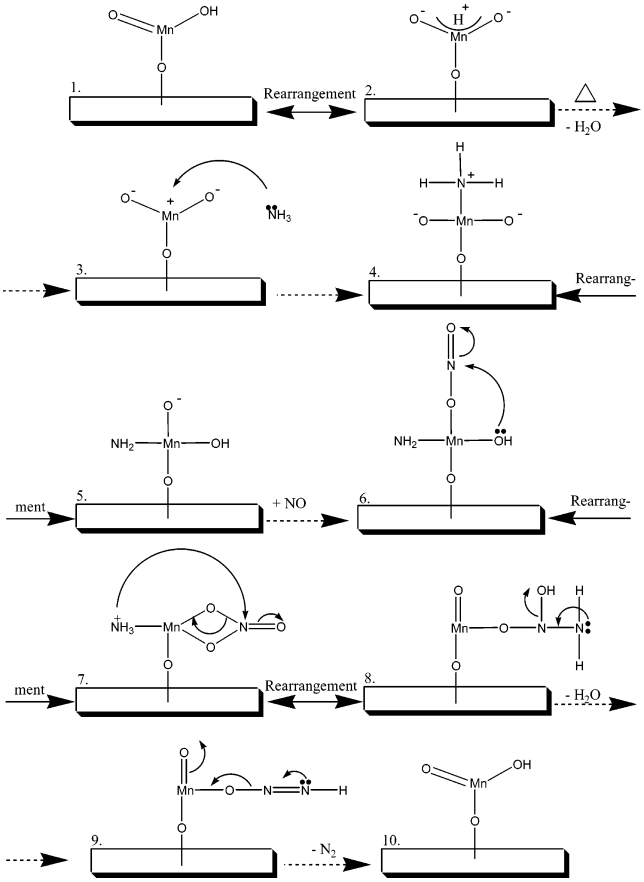

Figure 11. Proposed reaction mechanism for the selective catalytic reduction of NO with NH_3 over Mn/TiO_2 at low temperature.

All of this information has been used to propose a reaction mechanism for the SCR of NO with NH_3 at low temperature for manganese oxide supported on TiO_2, which has been shown to have high activity.[11] The reaction mechanism was proposed, based on the adsorption of NH_3 followed by NO over unidentate manganese oxide on TiO_2 hombikat support. According to Roozeboom et al.[38] and Schraml et al.,[39] several transition metals can form different types of isolated metal oxides on the support surface. This happens when the metal oxide loading is below or near monolayer coverage. In these cases, the active species can occur in general in every possible configuration (unidentate or bidentate or tridentate). For Mn loadings below monolayer coverage on the TiO_2 support, the only possible forms are either unidentate or bidentate. Therefore, the mechanism shown in Figure 11 was proposed with respect to the isolated unidentate MnO_2 form. The mechanism shows the reaction commencing with the adsorption of NH_3 onto the Lewis acid sites of Mn^{4+}. In particular, the active sites are believed to be the Lewis acid sites that correspond to the lower split speak of $\delta_s(NH_3)$ ($\sim$1170 cm^{-1}) that immediately react with NO and disappear. Although the formation of amide species was observed over the TiO_2 support, the FTIR data for 5 wt % Mn/TiO_2 did not provide conclusive proof of them. Nevertheless, hydrogen abstraction has been reported to occur over supported MnO_x catalysts before, and the case of overzealous hydrogen abstraction has even been suggested to lead to N_2O formation.[28] This provides support for the inclusion of amine species into the reaction mechanism. It is then proposed that the active amide species formed are capable of reacting with the bidentate nitrates ($\sim$1620 cm^{-1}) that developed. At this stage, it is proposed that the reaction mechanism proceeds through the formation of nitrosamide and azoxy species. While these species were not explicitly observed during the in situ FT-IR experiments, their absence does not rule out their possible formation, as they may have very short lifetimes as reaction intermediates. The products, N_2 and H_2O, are released and the original active site is regenerated to continue participating in the reaction. The species involved during the mechanism are all capable of forming over oxides of Cu as well; however, the reactive nature of the surface prevented the accurate assignment of peaks to species adsorbed on the surface. As a result, it is possible that supported Cu oxides may follow the same mechanism as well. The disappearance of Brønsted acid sites over 20 wt % Cr/TiO_2 after the introduction of NO sharply contrasts the behavior of Mn and Cu, suggesting that a different reaction pathway is involved. Whether Cr/TiO_2 follows a previously established mechanism that relies on Brønsted acid sites or a completely new one at these conditions is debatable, and that topic is the subject of undergoing work in our group.

Conclusions

Ammonia and nitric oxide were adsorbed or coadsorbed onto the surfaces of TiO_2, MnO_x/TiO_2, CrO_x/TiO_2, and CuO_x/TiO_2. The adsorption of NH_3 revealed the presence of Lewis acid sites over all of the materials tested, but the split peak of the symmetric deformation of NH_3 coordinated to Lewis acid sites was absent in CrO_x/TiO_2. Both the $\delta_s(NH_3)$ and $\delta_{as}(NH_3)$ forms of NH_3 coordinated to Lewis acids sites were observed, although the latter species was not observed over TiO_2. The adsorption strength of NH_3 indicated by $\delta_s(NH_3)$ decreased in the order Ti > Mn > Cr $\sim$ Cu, while the adsorption strength of NH_3 indicated by $\delta_{as}(NH_3)$ decreased in the order Mn > Cr $\sim$ Cu. CrO_x/TiO_2 was the only material tested that generated meaningful amounts of Brønsted acidity, as the stronger Brønsted acid sites observed over the other materials were generated from impurities present on the TiO_2. Nitric oxide was able to adsorb onto the surface of all the materials tested, even in the absence of oxygen. The formation of nitrates indicated the readily available lattice oxygen in all of the materials tested. Monodentate and bidentate nitrates formed on the surface of all the materials, and the relative strengths decreased in the following order for both cases: Ti > Mn $\sim$ Cu > Cr. Bridged nitrates only formed on the surface of 20 wt % Cr/TiO_2.

The FTIR data collected has been used to propose a reaction mechanism for the SCR of NO with NH_3 at low temperature. A combination of moderately strong monodentate and bidentate nitrate species, along with a split in the symmetric deformation of NH_3 coordinated to Lewis acid sites, appear to be important for high activity and selectivity for low-temperature SCR with NH_3. The specific Lewis acid sites located at $\sim$1170 cm^{-1}, which correspond to the lower split peak of $\delta_s(NH_3)$, are believed to be important in facilitating hydrogen abstraction to form amide species that react with bidentate nitrates (1620 cm^{-1}). It is proposed that the reaction mechanism proceeds through the formation of nitrosamide and azoxy species, which most likely possess lifetimes as reaction intermediates that are too brief for detection. This pathway has been proposed primarily for MnO_x/TiO_2 catalysts, although it may hold for CuO_x/TiO_2 as well. In contrast, the apparent participation of Brønsted acid sites for CrO_x/TiO_2 suggests that a different reaction pathway is involved, which is the subject of ongoing research.

Acknowledgment. The authors are grateful to the Ohio Coal Development Office (OCDO) for providing financial support and allowing us to publish the findings.

References and Notes

(1) Bosch, H.; Janssen, F. *Catal. Today* **1988**, *2*, 369.
(2) Topsøe, N.-Y. *Cattech* **1997**, *1*, 125.
(3) Inomata, M.; Miyamoto, A.; Murakami, Y. *J. Catal.* **1980**, *62*, 140.
(4) Janssen, F.; van den Kerkhof, F.; Bosch, H. *J. Phys. Chem.* **1987**, *91*, 5921.
(5) Wood, S. C. *Chem. Eng. Prog.* **1994**, *90*, 32.
(6) Dumesic, J. A.; Topsøe, N.-Y.; Topsøe, H.; Slabiak, T. *J. Catal.* **1996**, *163*, 409.
(7) Grzybeck, T.; Klinik, J.; Rogoz, M.; Papp, H. *J. Chem. Soc. Faraday Trans.* **1998**, *94*, 2843.
(8) Zhu, Z.; Liu, Z.; Liu, S.; Niu, H. *Appl. Catal., B: Environ.* **1999**, *23*, L229.
(9) Singoredjo, L.; Korver, R.; Kapteijn, F.; Moulijn, J. *Appl. Catal., B: Environ.* **1992**, *1*, 297.
(10) Armor, J. Environmental Catalysis. Presented at the 205th National Meeting of the American Chemical Society, 1994.
(11) Smirniotis, P. G.; Peña, D. A.; Uphade, B. S. *Angew. Chem. Int. Ed. Engl.* **2001**, *40*, 2479.
(12) Takagi, M.; Kawai, T.; Soma, M.; Onishi, T.; Tamaru, K. *J. Catal.* **1977**, *50*, 441.
(13) Miyamoto, A.; Yamazaki, Y.; Hattori, T.; Inomata, N.; Murakami, Y. *J. Catal.* **1982**, *74*, 144.
(14) Rajadhyksha, R. A.; Knözinger, H. *Appl. Catal.* **1989**, *51*, 81.
(15) Dines, T. J.; Rochester, C. H.; Ward, A. M. *J. Chem. Soc., Faraday Trans.* **1991**, *87*, 1473.
(16) Topsøe, N.-Y. *J. Catal.* **1991**, *128*, 499.
(17) Topsøe, N.-Y. *Science* **1994**, *265*, 1217.
(18) Topsøe, N.-Y.; Topsøe, H.; Dumesic, J. A. *J. Catal.* **1995**, *151*, 226.
(19) Topsøe, N.-Y.; Dumesic, J. A.; Topsøe, H. *J. Catal.* **1995**, *151*, 241.
(20) Centeno, M. A.; Carrizosa, I.; Odrizola, J. A. *Appl. Catal., B: Environ.* **2001**, *29*, 307.
(21) Busca, G.; Lietti, L.; Ramis, G.; Berti, F. *Appl. Catal., B: Environ.* **1998**, *18*, 1.
(22) Ramis, G.; Busca, G.; Bregani, F.; Forzatti, P. *Appl. Catal.* **1990**, *64*, 259.
(23) Amores, J. M. G.; Escribano, V. S.; Ramis, G.; Busca, G. *Appl. Catal., B: Environ.* **2001**, *13*, 45.
(24) Ramis, G.; Yi, L.; Busca, G. *Catal. Today* **1996**, *28*, 373.
(25) Schraml-Marth, M.; Wokaun, A.; Curry-Hyde, H. E.; Baiker, A. *J. Catal.* **1992**, *133*, 415.
(26) Schraml-Marth, M.; Wokaun, A.; Curry-Hyde, H. E.; Baiker, A. *J. Catal.* **1992**, *133*, 431.
(27) Schraml-Marth, M.; Wokaun, A.; Baiker, A. *J. Catal.* **1992**, *138*, 306.
(28) Kapteijn, F.; Singoredjo, L.; van Driel, M.; Andreïni, A.; Moulijn, J. A.; Ramis, G.; Busca, G. *J. Catal.* **1994**, *150*, 105.
(29) Kijlstra, W. S.; Brands, D. S.; Poels, E. K.; Bliek, A. *J. Catal.* **1997**, *171*, 208.
(30) Stoilova, D.; Cheshkova, K.; Nickolov, R. *React. Kinet. Catal. Lett.* **1998**, *65*, 265.
(31) Lietti, L.; Ramis, G.; Berti, F.; Toledo, G.; Robba, D.; Busca, G.; Forzatti, P. *Catal. Today* **1998**, *42*, 101.
(32) Matralis, H.; Ciardelli, M.; Ruwet, M.; Grange, P. *J. Catal.* **1995**, *157*, 368.
(33) Amores, J. M. G.; Escribano, V. S.; Ramis, G.; Busca, G. *Appl. Catal., B: Environ.* **1997**, *13*, 45.
(34) Ramis, G.; Busca, G.; Turco, M.; Kotur, E.; Willey, R. J. *J. Catal.* **1995**, *157*, 523.
(35) Valyon, J.; Hall, W. K. *J. Phys. Chem.* **1993**, *97*, 1204.
(36) Kugler, E. L.; Kadet, A. B.; Gryder, J. W. *J. Catal.* **1976**, *41*, 72.
(37) Kantcheva, M. *J. Catal.* **2001**, *204*, 479.
(38) Roozeboom, F.; Mittlemeyer-Hazeleger, M. C.; Moulijn, J. A.; Medema, T.; de Beer, V. H. J.; Gellings, P. J. *J. Phys. Chem.* **1980**, *84*, 2783.
(39) Schraml, M.; Fluhr, W.; Wokaun, A.; Baiker, A. *Ber. Bunsen-Ges. Phys. Chem.* **1989**, *93*, 852−857.